Pressure Loss in Unsteady Annular Channel Flow

Enrico Pasquini*, Heiko Baum* and Hubertus Murrenhoff**

FLUIDON GmbH, Jülicher Str. 338a, D-52070 Aachen, Germany*
RWTH Aachen University, Institute for Fluid Power Drives and Systems (IFAS), Campus Boulevard 30, D-52074 Aachen, Germany**
E-Mail: enrico.pasquini@fluidon.com

The paper presents a methodology for calculating the pressure loss in unsteady flows through concentric annular channels. The momentum equation in axial direction is solved in the Laplace domain to obtain the unsteady radial velocity distribution. Based on the velocity profile, the relation between the Laplace transforms of pressure loss and area-averaged flow velocity is derived. A time domain representation of this equation is provided for harmonically oscillating flows. For arbitrary temporal distributions of the flow, the inverse Laplace transform of the relation between pressure loss and flow velocity has to be derived. Since finding the inverse Laplace transform of the exact weighting function for each possible radius ratio is cumbersome, the annular channel flow is approximated by a plane channel. An error analysis shows that this approximation introduces errors less than 1 % for channel geometries down to radius ratios of 0.45. The approximated weighting function is transformed into the time domain by using the residue theorem from complex analysis. The resulting convolution integral can be used in one-dimensional hydraulic system simulation software.

Keywords: concentric annular channel, frequency-dependent friction, unsteady flow, hydraulic simulation
Target audience: Design Process

1 Introduction

An annular channel is formed if a cylinder (radius r_i) is mounted in a pipe (inner radius r_o), see Figure 1. The present paper is limited to concentric annular channels, i.e. the axis of the pipe and the axis of the cylinder always coincide. Annular channels appear in various engineering applications ranging from tube heat exchangers to spool valve clearances. A key parameter to characterize annular channels is the ratio $\varrho = r_i/r_o$ of the cylinder radius and the pipe's inner radius. Since in most hydraulic engineering applications the gap height $h = r_o - r_i$ is very small (e.g. few micrometres in sealing gaps), the radius ratio is typically close to unity.

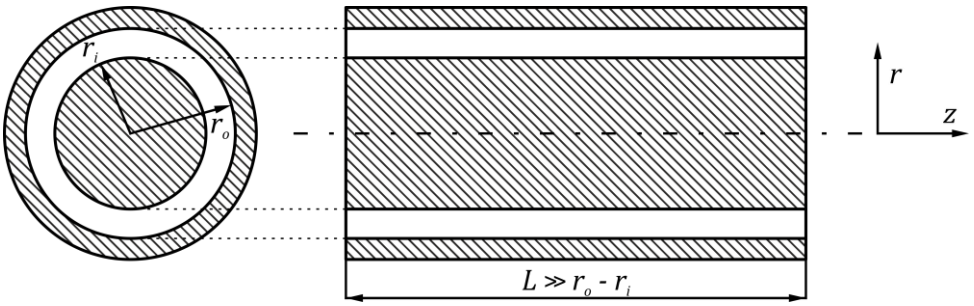

Figure 1: Geometry of a concentric annular channel.

A typical engineering problem with respect to annular channels is the calculation of the pressure loss Δp for a given flow rate Q or area-averaged velocity $\bar{u} = Q/A$. For laminar steady flow ($\partial\bar{u}/\partial t = 0$), an analytical

expression for the pressure loss is known, see e.g. IDELCHIK [1]. For unsteady laminar flow with a given temporal distribution of the flow rate, a reasonable first guess would be to take the instantaneous value $\bar{u}(t)$ and calculate the unsteady pressure loss based on this value. This method is referred to as the *quasi steady approach* and is a common practice not only for annular channels but for pipe flows in general. The quasi steady approach gives exact results for unsteady flows with relatively low frequencies. For highly dynamic flows like water hammer problems, the experiments conducted by HOLMBOE and ROULEAU [2] (performed with cylindrical pipes without an inner cylinder) could demonstrate that the quasi steady approach fails to predict the correct shape of the pressure transients, see Figure 2:

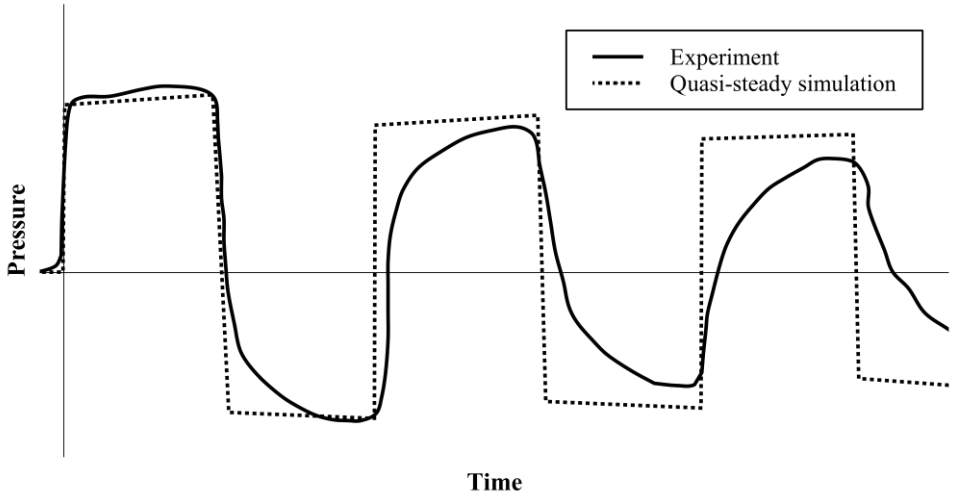

Figure 2: Pressure transients for a typical water hammer experiment [3].

As can be seen in the diagram, the quasi-steady approach significantly underestimates the unsteady pressure loss (and hence amplitude damping) during a water hammer event. In such cases of highly dynamic flow, the effect of so-called *frequency-dependent friction* has to be taken into account. If frequency-dependent friction is used in the simulation, the correct shape of the pressure transients is matched very well. For laminar flows through circular pipes without an inner cylinder, a universal method for taking frequency-dependent friction into account has been published by ZIELKE [3]. The respective solution for annular channels is derived in the subsequent sections.

2 Exact solution

The pressure loss in any channel flow depends on the velocity distribution over the cross section of the respective channel. Hence, in order to calculate the pressure loss in annular channels, the velocity distribution has to be obtained.

2.1 Radial velocity distribution

Assuming nearly incompressible flow through annular channels of constant cross-section, the resulting velocity field is fully described by the radial distribution of the axial component $u_z(r,t)$ of the flow velocity. For simplicity, this quantity will hereafter be addressed as $u(r,t)$ since there is no other relevant velocity component. The theoretical derivation of the radial velocity distribution is based on solving the momentum equation (NAVIER-STOKES equation) in the direction of the pipe axis. Taking the aforementioned assumptions into account, the momentum equation reduces to the following differential equation:

$$\frac{\partial u}{\partial t}+\frac{1}{\rho}\frac{\partial p}{\partial z}=\nu\left(\frac{\partial^2 u}{\partial r^2}+\frac{1}{r}\frac{\partial u}{\partial r}\right) \tag{1}$$

By performing a Laplace transform, the partial time derivative turns into an algebraic expression incorporating the Laplace variable s, which simplifies the equation further:

$$su^*+\frac{1}{\rho}\frac{\partial p^*}{\partial z}-\nu\left(\frac{\partial^2 u^*}{\partial r^2}+\frac{1}{r}\frac{\partial u^*}{\partial r}\right)=0 \tag{2}$$

Taking into account that the pressure does not depend on the radial coordinate, the equation above represents an ordinary differential equation. By introducing the non-dimensional radial coordinate $R=r\sqrt{s/\nu}$, this ODE can be transformed into a modified Bessel differential equation of zeroth order. The general solution reads:

$$u^*(R)=c_1 I_0(R)+c_2 K_0(R)-\frac{1}{s\rho}\frac{\partial p^*}{\partial z} \tag{3}$$

Here, I_0 and K_0 denote the modified Bessel functions of zeroth order. The constants c_1 and c_2 are chosen such that the no-slip condition is satisfied at the surfaces of the pipe and the cylinder:

$$u^*(R_i)=u^*(R_o)=0 \tag{4}$$

Applying these boundary conditions, the solution reads:

$$u^*(R)=\frac{1}{s\rho}\frac{\partial p^*}{\partial z}\left\{\frac{I_0(R)[K_0(R_o)-K_0(R_i)]-K_0(R)[I_0(R_o)-I_0(R_i)]}{I_0(R_i)K_0(R_o)-I_0(R_o)K_0(R_i)}-1\right\} \tag{5}$$

To simplify the representation of this expression in the subsequent sections, the following abbreviations are introduced:

$$\mathcal{I}_0=I_0(R_o)-I_0(R_i)=I_0(R_o)-I_0(\varrho R_o) \tag{6}$$

$$\mathcal{K}_0=K_0(R_o)-K_0(R_i)=K_0(R_o)-K_0(\varrho R_o)$$

$$\mathcal{N}_0=I_0(R_i)K_0(R_o)-I_0(R_o)K_0(R_i)=I_0(\varrho R_o)K_0(R_o)-I_0(R_o)K_0(\varrho R_o)$$

Using these abbreviations, the velocity profile can be expressed as:

$$u^*(R)=\frac{1}{s\rho}\frac{\partial p^*}{\partial z}\left[\frac{I_0(R)\mathcal{K}_0-K_0(R)\mathcal{I}_0}{\mathcal{N}_0}-1\right] \tag{7}$$

2.1.1 Steady flow

For the limit of steady flow ($s\to 0$), the velocity profile approaches the following expression:

$$\lim_{s\to 0}u^*(R)=u(r)=\frac{r_o^2}{4\eta}\frac{\partial p}{\partial z}\left[\left(\frac{r}{r_o}\right)^2+\frac{\ln\left(\frac{r}{r_o}\right)(1-\varrho^2)}{\ln\varrho}-1\right] \tag{8}$$

To generalize the representation of the velocity profile, it is expressed using a non-dimensional radial coordinate r'. This coordinate is defined in such a way that it assumes the values $r'=0$ at the cylinder's outer surface and $r'=1$ at the pipe wall:

$$r'=\frac{r-r_i}{r_o-r_i} \tag{9}$$

For the graphical representation of the radial velocity distribution, the flow velocity $u(r)$ is normalized with its maximum value u_{max}:

$$u' = \frac{u(r)}{u_{max}} \tag{10}$$

The velocity maximum $u'_{max} = 1$ is located at the coordinate r'_{max}:

$$r'_{max} = \frac{\sqrt{\frac{\varrho^2 - 1}{2\ln\varrho}} - \varrho}{1 - \varrho} \tag{11}$$

The normalized flow velocity u' for different radius ratios ϱ is plotted against the non-dimensional radial coordinate r' in Figure 3:

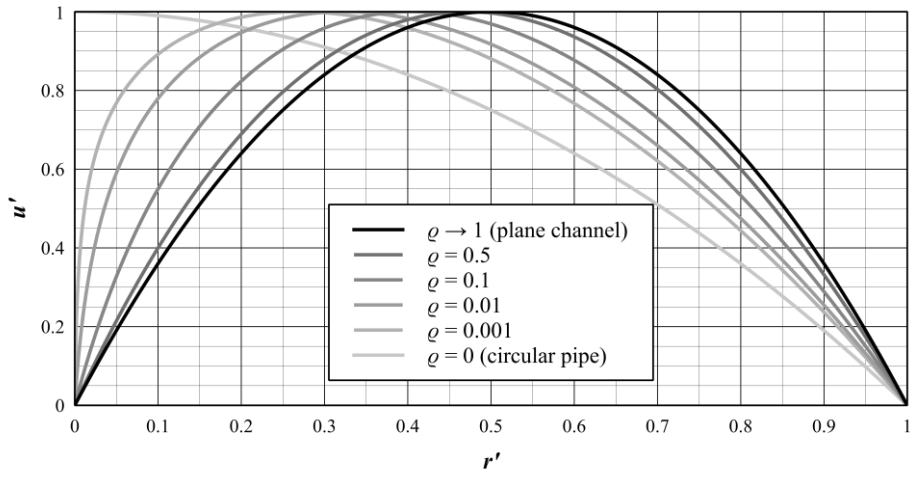

Figure 3: Non-dimensional radial velocity profile for steady laminar flow through annular ducts.

With vanishing gap height (ϱ→1), the velocity profile approaches a parabolic shape as it is known from the *plane channel POISEUILLE flow* between two parallel flat plates of infinite width. The velocity profiles for radius ratios $0.5 < \varrho < 1$ are not plotted separately since they virtually coincide with the velocity distribution of the plane channel. Accordingly, the velocity maximum moves towards the gap centre for $\varrho \to 1$:

$$\lim_{\varrho \to 1} r'_{\max} = \frac{1}{2} \tag{12}$$

2.1.2 Harmonically oscillating flow

The volume flow Q and the area-averaged velocity $\bar{u}^*$ are obtained by integrating the velocity profile over the flow area $A = \pi(r_o^2 - r_i^2)$:

$$\bar{u}^* = \frac{Q^*}{A} = \frac{1}{A}\int_A u^* \,\mathrm{d}A = \frac{2\pi}{\pi r_o^2(1-\varrho^2)}\int_{r_i}^{r_o} u^* r \,\mathrm{d}r = \frac{1}{s\rho}\frac{\partial p^*}{\partial z}\left[\frac{2(\mathcal{I}_1\mathcal{K}_0 + \mathcal{I}_0\mathcal{K}_1)}{(1-\varrho^2)R_o\mathcal{N}_0} - 1\right] \tag{13}$$

Here, the following abbreviations were used:

$$\mathcal{I}_1 = I_1(R_o) - \varrho I_1(\varrho R_o) \tag{14}$$

$$\mathcal{K}_1 = K_1(R_o) - \varrho K_1(\varrho R_o)$$

Combining equations 7 and 13, one obtains the radial velocity distribution as a function of the mean flow rate:

$$u^*(R) = \bar{u}^* \frac{I_0(R)\mathcal{K}_0 - K_0(R)\mathcal{I}_0 - \mathcal{N}_0}{\frac{2(\mathcal{I}_1\mathcal{K}_0 + \mathcal{I}_0\mathcal{K}_1)}{(1-\varrho^2)R_o} - \mathcal{N}_0} \tag{15}$$

The velocity profile for unsteady flow depends on the Laplace variable s. For the analysis of harmonically oscillating flows, s can be replaced by $i\omega$. Instead of the angular frequency ω, the non-dimensional gap WOMERSLEY number Wo_h is used. Unlike the usual definition of the WOMERSLEY number Wo, the gap WOMERSLEY number is calculated by replacing the diameter with the hydraulic diameter d_h of the annular channel ($d_h = 2h$):

$$Wo_h = \frac{d_h}{2}\sqrt{\frac{\omega}{\nu}} = h\sqrt{\frac{\omega}{\nu}} = (r_o - r_i)\sqrt{\frac{\omega}{\nu}} \tag{16}$$

The non-dimensional radial velocity profile $u' = u^*(R)/u^*_{\max}$ for harmonically oscillating annular channel flows is plotted for gap WOMERSLEY numbers $1 \leq Wo_h \leq 100$ in Figure 4:

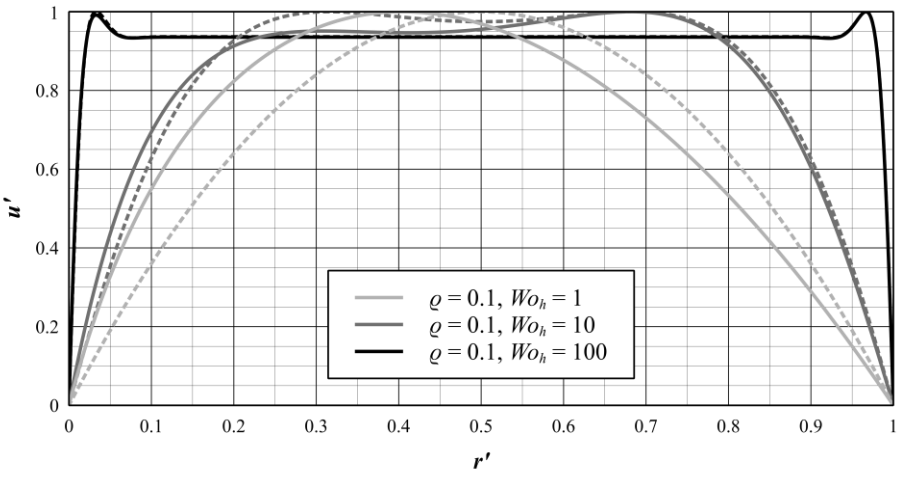

Figure 4: Unsteady radial velocity profile for harmonically oscillating laminar flow through annular channels.

As can be seen, the differences between the velocity distributions of the annular channel with a radius ratio of $\varrho = 0.1$ and the plane channel ($\varrho \to 1$, dotted lines) are large for small gap WOMERSLEY numbers. Both velocity profiles practically coincide with their steady flow counterparts from Figure 3. With increasing Wo_h, the deviation between the velocity distributions becomes smaller. For large gap WOMERSLEY numbers $Wo_h = 100$, the velocity profiles of the plane and annular channel ($\varrho = 0.1$) are virtually indistinguishable. Hence, even channels with quite small radius ratios behave like a plane channel at sufficiently high frequencies. It should be noted that the velocity maxima move towards the walls with increasing gap WOMERSLEY number. This phenomenon is known as the RICHARDSON annular effect from pipes without an inner cylinder [4].

2.2 Pressure loss as a function of area-averaged velocity

The pressure loss per unit length is the result of the shear stresses τ_i^* and τ_o^* acting at the cylinder and pipe walls:

$$\pi(r_o^2 - r_i^2)\frac{\Delta p^*}{\Delta z} = \pi(r_i\tau_i^* + r_o\tau_o^*) \tag{17}$$

The shear stresses are proportional to the gradient of the velocity profile at the wall:

$$\tau_i^* = \eta \left.\frac{\partial u^*}{\partial r}\right|_{r=r_i} \tag{18}$$

$$\tau_o^* = -\eta \frac{\partial u^*}{\partial r}\bigg|_{r=r_o}$$

Combining equations 13, 17 and 18, one obtains the following relation between the unsteady pressure loss per unit length and the area-averaged velocity:

$$\frac{\Delta p^*}{\Delta z} = \frac{\eta}{r_o^2} \frac{R_o^2}{\frac{(1-\varrho^2) R_o \mathcal{N}_0}{2(\mathcal{J}_1 \mathcal{K}_0 + \mathcal{J}_0 \mathcal{K}_1)} - 1} \bar{u}^* = \frac{\eta}{r_o^2} F^* \bar{u}^* \tag{19}$$

Here, $F^*(s)$ denotes a non-dimensional function in which all frequency-dependent characteristics of the pressure loss are concentrated.

2.2.1 Steady flow

For the limit of steady flow, equation 19 converges towards the following expression:

$$\lim_{s \to 0} \frac{\Delta p^*}{\Delta z} = \frac{\Delta p}{\Delta z} = \frac{\eta}{r_o^2} \frac{8}{1 + \varrho^2 + \frac{(1-\varrho^2)}{\ln \varrho}} \bar{u} \tag{20}$$

For vanishing relative gap height ($\varrho \to 1$), the pressure loss law equals the one of a plane channel of the same gap height h:

$$\lim_{\varrho \to 1} \frac{\Delta p}{\Delta z} = \frac{\eta}{h^2} \frac{8(1-\varrho)^2}{1 + \varrho^2 + \frac{(1-\varrho^2)}{\ln \varrho}} \bar{u} = \frac{12\eta}{h^2} \bar{u} \tag{22}$$

2.2.2 Harmonically oscillating flow

If $\bar{u}(t)$ is assumed to be harmonically oscillating (e.g. like the flow provided by a reciprocating pump), equation 19 can be easily transformed into the time domain. Assuming a temporal variation of the mean flow velocity of the form $\bar{u}(t) = \bar{u}_0 \sin(\omega t)$, the pressure loss per unit length is given by the following equation:

$$\frac{\Delta p(t)}{\Delta z} = V \frac{\Delta p_0}{\Delta z} \sin(\omega t + \varphi) = V \frac{\eta}{r_o^2} \frac{8}{1 + \varrho^2 + \frac{(1-\varrho^2)}{\ln \varrho}} \bar{u}_0 \sin(\omega t + \varphi) \tag{23}$$

Here, $\Delta p_0 / \Delta z$ refers to the pressure loss per unit length calculated by inserting $\bar{u}_0$ into equation 20 (quasi-steady approach). The magnification factor V and the phase angle φ are plotted against the gap WOMERSLEY number Wo_h in Figures 5 and 6:

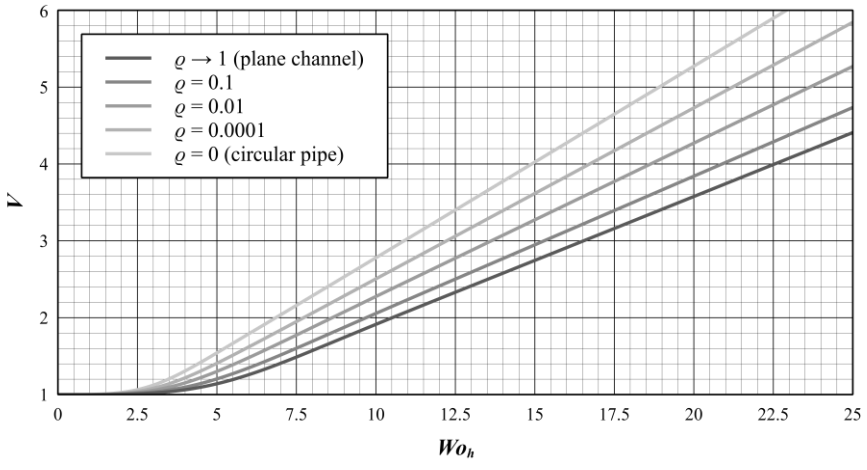

Figure 5: Magnification factor versus gap Womersley number for harmonically oscillating laminar flow.

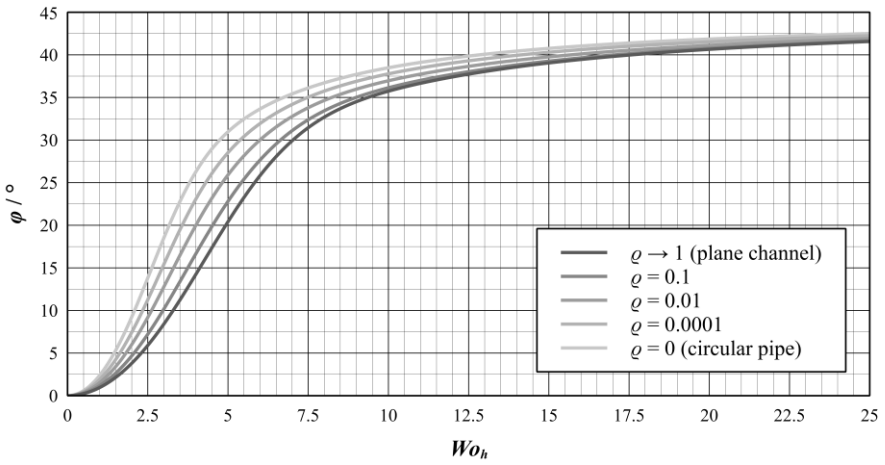

Figure 6: Phase angle versus gap Womersley number for harmonically oscillating laminar flow.

If the oscillation frequency ω is smaller than ν/h^2 (i.e. $Wo_h < 1$), the magnification factor tends to unity and the phase angle vanishes. For this case, the quasi-steady approach provides exact results:

$$\frac{\Delta p(t)}{\Delta z} = \frac{\Delta p_0}{\Delta z}\sin(\omega t) \tag{24}$$

For large frequencies $\omega \to \infty$, the phase angle approaches $\varphi \to 45°$. The respective magnification factor grows monotonously to $V \to \infty$. Hence, the influence of frequency-dependent friction on highly dynamic flows cannot be neglected.

2.3 Arbitrary unsteady flows

For unsteady flows with a given velocity distribution $\bar{u}(t)$ of arbitrary shape, derivation of the time domain formulation of equation 19 requires more effort. Since the pressure loss per unit length is given as a product of two functions in the Laplace domain, the respective time domain expression will feature a convolution integral of the following form:

$$\frac{\Delta p}{\Delta z} = \frac{\eta}{r_o^2}\int_0^t \bar{u}(t_1)F(t-t_1)\,\mathrm{d}t_1 \tag{25}$$

To evaluate this integral, the inverse Laplace transform of $F^*(s)$ has to be derived. A necessity for the existence of the inverse of a Laplace transform is the convergence of the Laplace transform to zero for $s \to \infty$. Examination of F^* reveals that this function does not converge to zero for $s \to \infty$. However, if the pressure loss is assumed to be a product of the time derivative $s\bar{u}^*$ of the averaged flow velocity and the function F^*/s, an inverse Laplace transform exists. Hereafter, the quotient F^*/s will be abbreviated by W^*, which is given by:

$$W^*(s) = \frac{2r_o^2/\nu}{\dfrac{R_o(1-\varrho^2)[I_0(\varrho R_o)K_0(R_o) - I_0(R_o)K_0(\varrho R_o)]}{[I_1(R_o) - \varrho I_1(\varrho R_o)][K_0(R_o) - K_0(\varrho R_o)] + [K_1(R_o) - \varrho K_1(\varrho R_o)][I_0(R_o) - I_0(\varrho R_o)]} - 2} \tag{26}$$

Since partial fraction decomposition is not possible due to the transcendental nature of the so-called *weighting function* $W^*(s)$, the general inversion formula (the *BROMWICH integral*) has to be employed in order to obtain the time domain representation $W(t)$:

$$W(t) = \mathcal{L}^{-1}\{W^*(s)\}(t) = \frac{1}{2\pi i}\int_{\gamma-i\infty}^{\gamma+i\infty} \mathrm{e}^{st}W^*(s)\,\mathrm{d}s \tag{27}$$

This integral can be solved by using the *residue theorem* from complex analysis. The residue theorem states that the contour integral along a closed curve equals the sum of the residues of the integrand:

$$\frac{1}{2\pi i}\int_{\gamma-i\infty}^{\gamma+i\infty} \mathrm{e}^{st}W^*(s)\,\mathrm{d}s = \sum_{j=0}^{n} \mathrm{Res}\{\mathrm{e}^{st}W^*(s)\}_{s=s_j} \tag{28}$$

If the integrand of the contour integral can be represented as a quotient of two functions $\mathcal{X}(s)$ and $\mathcal{Y}(s)$, the residue at a simple pole $s = s_j$ is given by:

$$\mathrm{Res}\left\{\frac{\mathcal{X}(s)}{\mathcal{Y}(s)}\right\}_{s=s_j} = \frac{\mathcal{X}(s_j)}{\left.\frac{\partial \mathcal{Y}}{\partial s}\right|_{s=s_j}} \tag{29}$$

Hence, in order to evaluate the integral, the derivative of the denominator of $W^*(s)$ has to be evaluated at the poles s_j. Analysis of the weighting function shows that the first (and trivial) singularity is located at $s_0 = 0$. All other poles are on the negative real axis. Since the weighting function is dependent on the ratio ϱ, the positions of the poles vary with this parameter, too. It can be shown that for the technically important limit $\varrho \to 1$ (sealing gaps), the position of the first nontrivial pole tends to $s_1 \to -\infty$. This behaviour represents a serious hindrance for the numerical evaluation of the weighting function. Therefore, the exact solution for the annular channel is replaced by the plane channel approximation.

3 Plane channel approximation

The discussion of the steady flow velocity profile in section 2.1.1 revealed that the velocity profile of annular channel flows converges to a parabolic shape if the radius ratio ϱ approaches unity. For the limiting case $\varrho \to 1$, the relation between pressure loss and area-averaged flow converges to the expression for plane channels as well. Hence, the annular channel with a radius ratio close to unity can be thought of as a perturbed variant of the plane channel. Based on this interpretation, the plane channel approximation is developed.

3.1 Velocity profile

Compared to the exact differential equation, the momentum equation of the plane channel approximation lacks a viscous term on the right hand side which represents the effects of the curvature of the velocity profile. Since a Cartesian coordinate system is used for the plane channel approximation, the radial coordinate r is replaced with the vertical coordinate y:

$$su^* + \frac{1}{\rho}\frac{\partial p^*}{\partial z} = \nu\frac{\partial^2 u^*}{\partial y^2} \tag{30}$$

The general solution of this differential equation reads:

$$u^*(Y) = c_1 \sinh Y + c_2 \cosh Y - \frac{1}{s\rho}\frac{\partial p^*}{\partial z} \tag{31}$$

In the general solution, the non-dimensional y-coordinate was used:

$$Y = y\sqrt{\frac{s}{\nu}} \tag{32}$$

Application of the no-slip condition at $y = h/2$ and $y = -h/2$ leads to the velocity profile:

$$u^*(Y) = \frac{1}{s\rho}\frac{\partial p^*}{\partial z}\left[\mathrm{sech}\left(\frac{H}{2}\right)\cosh Y - 1\right] \tag{33}$$

Here, H denotes the non-dimensional gap height $H = h\sqrt{s/\nu}$. For the limit of steady flow, the parabolic velocity profile is obtained as expected:

$$\lim_{s\to 0} u^*(Y) = u(y) = \frac{1}{2\eta}\frac{\partial p}{\partial z}\left(y^2 - \frac{h^2}{4}\right) \tag{34}$$

3.2 Pressure loss as a function of the area-averaged velocity

Based on the velocity profile, the pressure loss can be given as a function of the area-averaged velocity $\bar{u}^*$. The pressure loss for plane channels depends on the inner and outer shear stresses as follows:

$$\frac{\Delta p^*}{\Delta z} = \frac{\tau_i^* + \tau_o^*}{h} \tag{35}$$

The shear stresses are given by:

$$\tau_i^* = \eta \left.\frac{\partial u^*}{\partial y}\right|_{y=-\frac{h}{2}} \tag{36}$$

$$\tau_o^* = \eta \left.\frac{\partial u^*}{\partial y}\right|_{y=\frac{h}{2}}$$

Inserting these definitions into equation 35, we obtain the following relation between pressure loss per unit length and the pressure gradient:

$$\frac{\Delta p^*}{\Delta z} = -\frac{2}{H}\tanh\left(\frac{H}{2}\right)\frac{\partial p^*}{\partial z} \tag{37}$$

The area-averaged velocity is given by:

$$\bar{u}^* = \frac{1}{A}\int_A u^*\,\mathrm{d}A = \frac{1}{h}\int_{-\frac{h}{2}}^{\frac{h}{2}} u^*\,\mathrm{d}y = \frac{1}{s\rho}\frac{\partial p^*}{\partial z}\left[\frac{2}{H}\tanh\left(\frac{H}{2}\right) - 1\right] \tag{38}$$

Combining the two equations above gives the approximated relation between pressure loss and average velocity:

$$\frac{\Delta p^*}{\Delta z} = \frac{\eta}{h^2}\frac{h^2\frac{s}{\nu}}{\frac{h}{2}\sqrt{\frac{s}{\nu}}\coth\left(\frac{h}{2}\sqrt{\frac{s}{\nu}}\right) - 1}\bar{u}^* = \frac{\eta}{h^2}W^* s\bar{u}^* \tag{39}$$

3.2.1 Steady flow

For the case of steady flow, the pressure loss is given by:

$$\lim_{s\to 0}\frac{\Delta p^*}{\Delta z} = \frac{\Delta p}{\Delta z} = \frac{12\eta}{h^2}\bar{u} \tag{40}$$

This result is consistent with equation 22 of the exact solution.

3.2.2 Arbitrary unsteady flows

For the plane channel approximation, a universal inverse Laplace transform of the weighting function can be provided. The approximated weighting function is given by:

$$W^*(s) = \frac{h^2/\nu}{\frac{h}{2}\sqrt{\frac{s}{\nu}}\coth\left(\frac{h}{2}\sqrt{\frac{s}{\nu}}\right) - 1} \tag{41}$$

Analysis of the approximated weighting function shows a trivial pole at $s_0 = 0$; the first 20 non-trivial poles s_j are summarized in table 1:

Table 1: The first 20 non-trivial poles s_j of the weighting function.

j	$-\frac{s_j h^2}{\nu}$	j	$-\frac{s_j h^2}{\nu}$	j	$-\frac{s_j h^2}{\nu}$	j	$-\frac{s_j h^2}{\nu}$
1	80.76293	6	1659.96027	11	5213.01906	16	10740.00596
2	238.71764	7	2212.65811	12	6160.50114	17	12082.27450
3	475.59933	8	2844.31396	13	7186.94136	18	13503.48582
4	791.43137	9	3554.92598	14	8292.33702	19	15003.67761
5	1186.21761	10	4344.49457	15	9476.68957	20	16582.79459

The distance between the roots of the poles approaches $\sqrt{s_{j+1}} - \sqrt{s_j} = 2\pi i\, \nu/h^2$. The poles are used to evaluate the residues. For the approximated weighting function, the residues are given by:

$$\mathrm{Res}\left\{\frac{h^2/\nu}{\frac{h}{2}\sqrt{\frac{s}{\nu}}\coth\left(\frac{h}{2}\sqrt{\frac{s}{\nu}}\right)}\mathrm{e}^{st}\right\}_{s=s_j} = \frac{8}{\frac{2}{h}\sqrt{\frac{\nu}{s_j}}\coth\left(\frac{h}{2}\sqrt{\frac{s_j}{\nu}}\right) - \mathrm{csch}^2\left(\frac{h}{2}\sqrt{\frac{s_j}{\nu}}\right)}\mathrm{e}^{s_j t} \tag{42}$$

For the trivial pole $s_0 = 0$, the residue is given by:

$$\mathrm{Res}\{\mathrm{e}^{st}W^*(s)\}_{s=0} = 12 \tag{43}$$

For all other poles s_j, the residue equals:

$$\mathrm{Res}\{\mathrm{e}^{st}W^*(s)\}_{s=s_j} = 8e^{s_j t} \tag{44}$$

Hence, the approximated weighting function in the time domain is given by:

$$W(t) = 12 + 8\sum_{j=1}^{\infty}\mathrm{e}^{s_j t} \tag{45}$$

Clearly, the weighting function can be decomposed into a constant part (quasi-steady approach) and a time-dependent part (frequency-dependent friction). The dynamic weighting function $W_d(t)$ is obtained if the constant part is subtracted from the weighting function:

$$W_d(t) = W(t) - 12 \tag{46}$$

Analysis of equation 45 shows that the sum of residues converges very slowly for small times. The behaviour for small times $t \to 0$ in the time domain corresponds to the behaviour for large values of the Laplace variable $s \to \infty$ in the Laplace domain. Hence, the dynamic weighting function is developed into a power series at $s \to \infty$ in order to obtain a more suitable time domain expression for small times. For large arguments s, the hyperbolic cotangent tends faster towards unity than s tends towards infinity. Using this fact, the power series reads:

$$\lim_{s\to\infty} W^*(s) = \frac{h^2/\nu}{\frac{h}{2}\sqrt{\frac{s}{\nu}} - 1} \approx 2h\sqrt{\frac{1}{s\nu}} + \frac{4}{s} + \frac{8}{h}\sqrt{\frac{\nu}{s^3}} + \frac{16}{h^2}\frac{\nu}{s^2} + \frac{32}{h^3}\sqrt{\frac{\nu^3}{s^5}} + \frac{64}{h^4}\frac{\nu^2}{s^3} + \frac{128}{h^5}\sqrt{\frac{\nu^5}{s^7}} + \cdots \tag{47}$$

The inverse Laplace transform of the dynamic weighting function is then given by:

$$W_d(t_n) = \frac{2}{\sqrt{\pi t_n}} - 8 + \frac{16}{\sqrt{\pi}}\sqrt{t_n} + 16t_n + \frac{128}{3\sqrt{\pi}}\sqrt{t_n}^3 + 32t_n^2 + \frac{1024}{15\sqrt{\pi}}\sqrt{t_n}^5 + \cdots \tag{48}$$

Here, t_n refers to the normalised time $t_n = t\nu/h^2$. For normalised times $t_n < 0.0023$, the above equation should be used instead of equation 45. The dynamic weighting function is plotted against the normalised time in Figure 7:

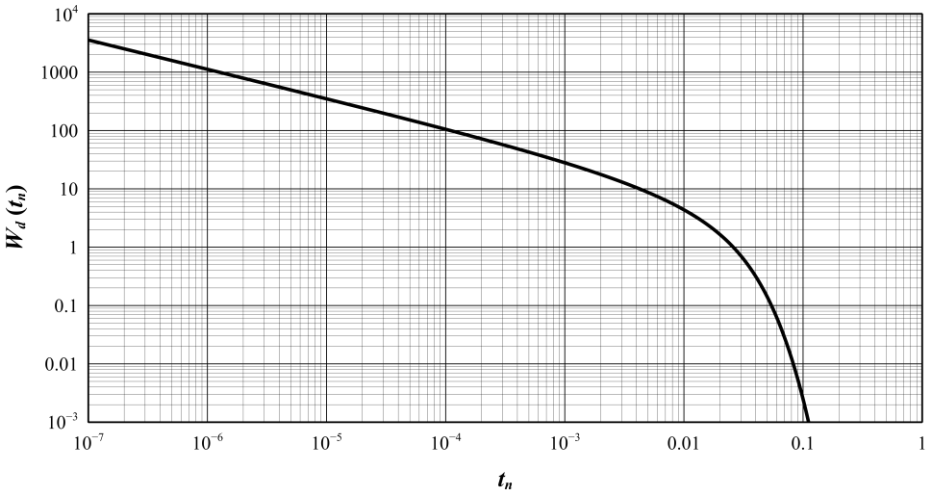

Figure 7: Dynamic weighting function versus normalised time.

Now that the dynamic weighting function is known, the overall pressure loss can be expressed as follows:

$$\frac{\Delta p(t)}{\Delta z} = \frac{12\eta}{h^2}\bar{u}(t) + \frac{\eta}{h^2}\int_0^t \frac{\partial \bar{u}}{\partial t}(t_1) W_d(t - t_1)\,\mathrm{d}t_1 \tag{47}$$

With this equation, all required information to calculate the pressure loss for a given temporal distribution of $\bar{u}(t)$ is provided. For practical calculations using a computer, the efficient approaches presented by TRIKHA [5] or SCHOHL [6] should be used.

3.3 Error Analysis

Due to the approximation by plane channel model, an error is introduced into the pressure loss calculation.

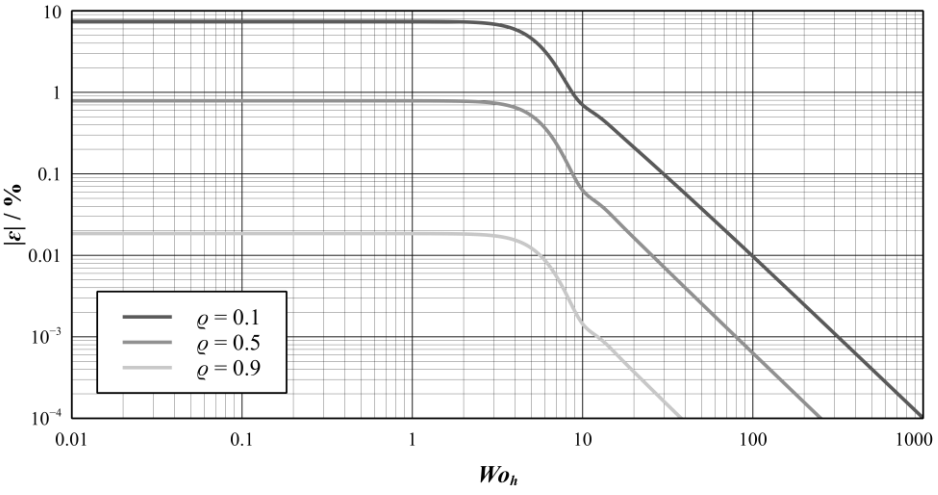

Figure 8: Relative error of the plane channel approximation versus gap Womersley number.

Since the pressure loss depends on the radius ratio ϱ, the relative error ε between the exact solution and the plane approximation will depend on this quantity as well. Since no time-domain expression for the exact relation between pressure loss and area-averaged velocity was derived, the comparison has to be carried out in the frequency domain. The relative error between the exact solution and the plane channel approximation is plotted against the gap WOMERSLEY number in Figure 8.

As can be seen, the maximum error occurs at low frequencies $Wo_h < 1$ and becomes smaller with increasing frequency. Hence, for analysing the maximum error as a function of the radius ratio, it is sufficient to limit the considerations to the error for the steady flow case. The maximum error is plotted against the radius ratio in Figure 9:

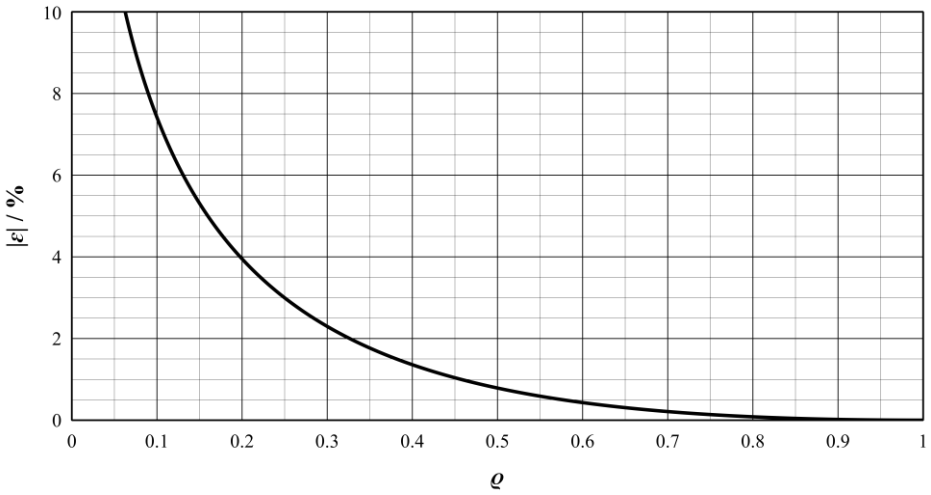

Figure 9: Relative error of the plane channel approximation versus radius ratio.

As can be seen in the diagram, the plane channel approximation introduces errors $\varepsilon < 1\,\%$ if the radius ratio is above $\varrho = 0.45$. This error can be decreased further if the quasi-steady part of the pressure loss is replaced by the exact expression (equation 20).

4 Summary and Conclusion

The findings of the paper can be summarized as follows:

- The pressure loss per unit length $\Delta p/\Delta z$ for steady laminar flow through an annular channel is given by:

$$\frac{\Delta p}{\Delta z} = \frac{\eta}{r_o^2} \frac{8}{1 + \varrho^2 + \frac{(1-\varrho^2)}{\ln \varrho}} \bar{u}$$

- The area-averaged flow velocity $\bar{u}$ is given by:

$$\bar{u} = \frac{Q}{A} = \frac{Q}{\pi r_o^2 (1-\varrho^2)}$$

- The pressure loss for steady flow through annular channels of vanishing gap height $h \to 0$ ($\varrho \to 1$) equals the pressure loss of a plane channel with the same gap height:

$$\frac{\Delta p}{\Delta z} = \frac{12\eta}{h^2} \bar{u}$$

- For oscillating pipe flow with $\bar{u}(t) = \bar{u}_0 \sin(\omega t)$, the pressure loss is given by:

$$\frac{\Delta p(t)}{\Delta z} = V \frac{\eta}{r_o^2} \frac{8}{1 + \varrho^2 + \frac{(1-\varrho^2)}{\ln \varrho}} \bar{u}_0 \sin(\omega t + \varphi)$$

- The magnification factor V and the phase angle φ are plotted as functions of the gap WOMERSLEY number in figures 5 and 6. The gap WOMERSLEY number is given by:

$$Wo_h = h\sqrt{\frac{\omega}{\nu}} = (r_o - r_i)\sqrt{\frac{\omega}{\nu}}$$

- For small angular frequencies $\omega < h^2/\nu$, the magnification factor V approaches unity and the phase angle φ tends to zero (quasi-steady limit).
- For arbitrary temporal distributions of the flow velocity, the pressure loss is given by a convolution integral. The convolution integral features a weighting function that depends on the radius ratio. Hence, a different inverse Laplace transform would have to be derived for each radius ratio. Instead, the annular channel flow is approximated by a plane channel model.
- The approximated pressure loss for arbitrary temporal distributions is given by:

$$\frac{\Delta p(t)}{\Delta z} = \frac{12\eta}{h^2}\bar{u}(t) + \frac{\eta}{h^2}\int_0^t \frac{\partial \bar{u}}{\partial t}(t_1) W_d(t - t_1)\,\mathrm{d}t_1$$

- The error due to plane channel approximation is largest for steady flow. For radius ratios $\varrho > 0.45$, the error is less than 1 %.
- For an efficient evaluation of the convolution integral, the methods presented by TRIKHA or SCHOHL should be used [5] [6].

Nomenclature

Variable	***Description***	***Unit***
A	Flow area	m²
$\coth(x)$	Hyperbolic cotangent of x	-
d_h	Hydraulic diameter, $d_h = 2h$	m
F	Function used in the determination of unsteady pressure loss	-
h	Gap height, $h = r_o - r_i$	m
H	Non-dimensional gap height, $H = h\sqrt{s/\nu}$	-
i	$\sqrt{-1}$	-
$I_n(x)$	Modified Bessel function of the first kind and nth order with the argument x	-
$K_n(x)$	Modified Bessel function of the second kind and nth order with the argument x	-
L	Length of the annular channel	m
p	Pressure	$kg \cdot m^{-1} \cdot s^{-2}$
r	Radial coordinate	m
r'	Non-dimensional radial coordinate	-
s	Laplace variable	s^{-1}

$\mathrm{sech}(x)$	Hyperbolic secant of x	-
t	Time coordinate	s
t_n	Normalised time	-
u	Axial component of the flow velocity	$m \cdot s^{-1}$
$\bar{u}$	Area-averaged flow velocity	$m \cdot s^{-1}$
u'	Non-dimensional oscillating velocity profile	-
W	Weighting function	-
W_d	Dynamic weighting function	-
Wo_h	Gap WOMERSLEY number	-
y	Cartesian coordinate for the plane channel model	m
Y	Non-dimensional y-coordinate, $Y = y\sqrt{s/\nu}$	-
z	Axial coordinate	m
ε	Error	%
η	Dynamic viscosity of the fluid	$kg \cdot m^{-1} \cdot s^{-1}$
ν	Kinematic viscosity of the fluid	$m^2 \cdot s^{-1}$
ϱ	Ratio of outer cylinder radius r_i and inner pipe radius r_o	-
ρ	Fluid density	$kg \cdot m^{-3}$
τ	Shear stress	$kg \cdot m^{-1} \cdot s^{-2}$
ω	Angular frequency	s^{-1}
x^*	Laplace-transform of the quantity x, $x^* = \mathcal{L}\{x\}(s)$	$[x]$

References

[1] IDELCHIK, I. E., *Handbook of hydraulic resistance*, 3rd Edition, 2003.

[2] HOLMBOE, E. L.; ROULEAU, W. T., *The effect of viscous shear on transients in liquid lines*, Journal of Basic Engineering, 1967, Vol. 89, No. 1, pp. 174-180.

[3] ZIELKE, Werner, *Frequency-dependent friction in transient pipe flow*, Journal of basic engineering, 1968, Vol. 90, No. 1, pp. 109-115.

[4] RICHARDSON, E. G.; TYLER, E., *The transverse velocity gradient near the mouths of pipes in which an alternating or continuous flow of air is established*. Proceedings of the Physical Society, 1929, Volume 42, No. 1, p. 1.

[5] TRIKHA, A. K., *An efficient method for simulating frequency-dependent friction in transient liquid flow*, Journal of Fluids Engineering, 1975, Vol. 97, No. 1, pp. 97-105.

[6] SCHOHL, G. A., *Improved approximate method for simulating frequency-dependent friction in transient laminar flow*, Transactions-American Society of Mechanical Engineers, Journal of Fluids Engineering, 1993, Vol. 115, pp. 420-420.